

Twisted one-dimensional charge transfer and related Y-shaped chromophores with a 4*H*-pyranylidene donor: synthesis and optical properties

Víctor Tejeda-Orusco,^a Raquel Andreu,^{a,*} Jesús Orduna,^a Belén Villacampa,^b Santiago Franco,^a Alba Civera^a.

^a Instituto de Nanociencia y Materiales de Aragón (INMA)-Departamento de Química Orgánica, CSIC-Universidad de Zaragoza, Zaragoza 50009, Spain.

^b Instituto de Nanociencia y Materiales de Aragón (INMA)-Departamento de Física de la Materia Condensada, CSIC-Universidad de Zaragoza, Zaragoza 50009, Spain.

Corresponding author: randreu@unizar.es

Dedicated to the memory of Dr. Thi-Thao Nguyen-Pipaud, good friend and warm-hearted colleague.

Abstract

Three series of push-pull derivatives bearing 4*H*-pyranylidene as electron donor group and a variety of acceptors were designed. On the one side, one dimensional chromophores with a thiophene ring (series **1H**) or 5-dimethylaminothiophene moiety (series **1N**) as auxiliary donor, non-coplanar with the π -conjugated system, were synthesized. On the other side, related two-dimensional (2D) Y-shaped chromophores (series **2**) were also prepared to compare how the diverse architectures affect the electrochemical, linear and second-order nonlinear optical (NLO) properties.

The presence of the 5-dimethylaminothiophene moiety in the exocyclic C=C bond of the pyranilidene unit gives rise to oxidation potentials rarely low, and the protonation (with an excess of trifluoroacetic acid) of its derivatives results in the apparition of a new blue-shifted band in the UV-visible.

The analysis of the properties of derivatives with and without the additional thiophene ring shows that this auxiliary donor leads to a higher NLO response, accompanied by an enhanced transparency.

Y-shaped chromophores of series **2** present a blue-shifted absorption, higher molar extinction coefficients and higher E_{ox} values compared to their linear twisted counterparts. As concerns NLO properties, 2D Y-shaped architecture gives rise to somewhat lower $\mu\beta$ values (except for thiobarbiturate derivatives)

Introduction

Second order nonlinear optical (NLO) materials¹ based on organic molecules have been investigated for long time due to their potential applications² related with second harmonic generation (SHG), optical switching, sensing,³ electro-optical (EO) modulation,⁴... Microscopic nonlinearities have been dramatically improved over time, and push-pull dipolar chromophores, with a Donor- π -Acceptor (D- π -A) structure and a suitable intramolecular charge transfer (ICT),⁵ have reached very high hyperpolarizability (β) values. The extent of the ICT can be delicately tuned by varying the components of this kind of molecules (D, π , and A), demonstrating to be essential to maximize the second-order NLO activity.⁵ Certainly, most applications require to transfer the molecular nonlinearity to the macroscopic level, looking for bulk materials with large NLO activity.^{1a,6}

The “construction” of new chromophores remains an interesting research topic. Focusing on the molecular design, two strategies have been used in recent times. On one hand,

multidimensional charge-transfer chromophores have been developed as a way to balance the nonlinearity-transparency trade-off arising from the strong push–pull structure, and to tune the ICT. Extraordinary arrangements of D-A chromophores that may be pictured as uppercase letters (molecules with shape similar to H, L, T, V, X, Y) appeared in the literature within the last few years.⁷ Furthermore, twisted ICT chromophores⁸ exhibit high hyperpolarizability compared to planar D–A molecules, showing to be a promising strategy for improving the microscopic nonlinearity of chromophores. Besides, these geometries hinder dipole aggregation at the macroscopic level.

Concerning donor units, the proaromatic character⁹ of pyranilidene moiety, and the subsequent gain in aromaticity along the ICT, has turned this fragment into a versatile building block, widening their use in the field of NLO,^{9,10} but also in different materials research areas such as dye-sensitized solar cells (DSSCs),¹¹ organic light-emitting diodes (OLEDs),¹² organic photovoltaics (OPV)¹³ or hole-transporting materials for perovskite solar cells,¹⁴ because the special electron-donating ability and chemical stability of this moiety.¹⁵

Having in mind the two approaches above mentioned (multidimensional charge-transfer and twisted chromophores) and taking advantage of our consolidated experience in the synthesis of D– π –A systems with the 4*H*-pyranilidene as donor moiety,^{9,10a,b,e,11b,15} we submit the design, synthesis and characterization of three series of molecules (Chart 1) for their study as second-order NLO chromophores. We have included in this analysis compounds **1Hb** and **2b**, two derivatives previously studied^{13b} as small donor molecules for OPV (see below).

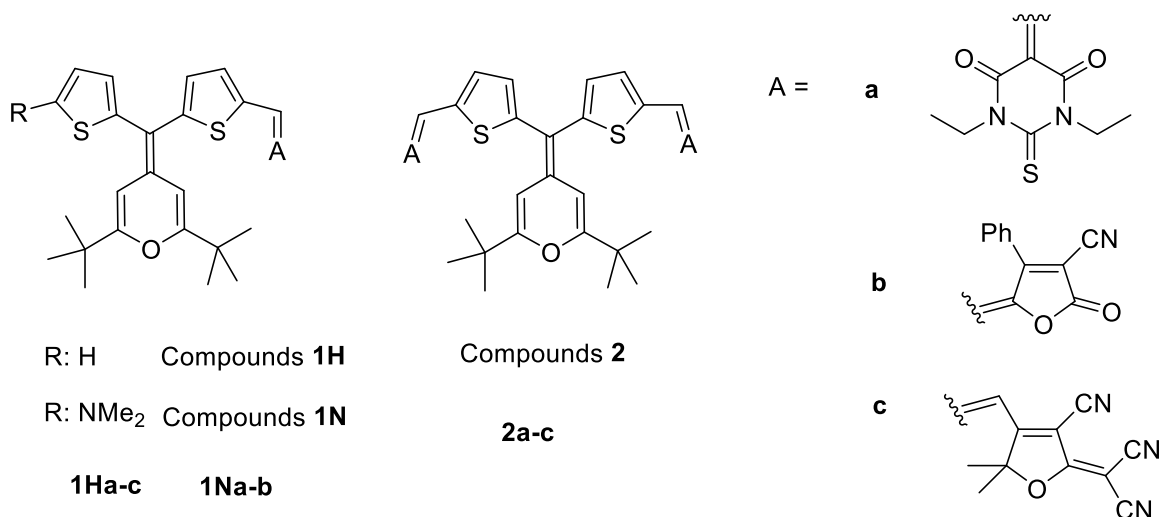


Chart 1. Molecular structures of the target compounds. Synthesis, cyclic voltammetry (CV) and UV studies in CH₂Cl₂ for compounds **1Hb** and **2b** in reference 13b.

As acceptor units, two common strong organic electron-withdrawing fragments like a thiobarbituric acid (derivatives **a**) and 2-dicyanomethylene-3-cyano-4,5,5-trimethyl-2,5-dihydrofuran (TCF) (derivatives **c**) were used, together with 4-phenyl-2-oxo-2,5-dihydrofuran-3-carbonitrile (derivatives **b**), a moderate acceptor that has given rise to an excellent matching of effective polarized chromophores with upgraded second-order NLO activity.^{10e}

For the chromophores **1H** and **1N**, the exocyclic C=C double bond of the 4*H*-pyranylidene donor is equipped with a thiophene (**1H**) or a 5-dimethylaminothiophene (**1N**) unit. These substituents have the following three features: i) they are necessarily not coplanar with the D–A system; ii) they could be considered as auxiliary donors¹⁶ and iii) they introduce steric hindrance. As a result, they can improve the electron-donating ability of 4*H*-pyranylidene moiety, also showing an isolating effect¹⁷ that hinders the antiparallel dipole-dipole orientations. Derivatives **2** can be considered as Y-shaped chromophores with the thiophene ring as π -spacer and the withdrawing group arranged around the central 4*H*-pyranylidene core. Both types of chromophores (**1H/1N** and **2**) summarize the two strategies explained above: to have a multidimensional ICT and twisted structures.

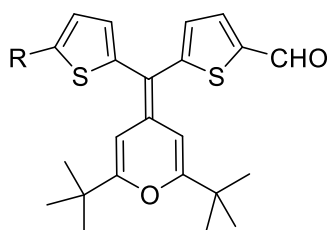
Related compounds to those proposed in Chart 1 have been previously reported by our group for other two different applications and the influence of the auxiliary thiophene ring has been explored: i) dyes designed for DSSCs analogous to **1H** compounds with cyanoacrylic acid as acceptor, gave rise to twisted structures preventing the formation of aggregates and, therefore, increasing the efficiency of the derived cells;^{11d} ii) compound **1Hb** and a related system with dicyanovinyl as electron-withdrawing end were studied as donor materials for OPV, leading to poor efficiencies due to the fact that the twisted structure prevents the formation of suitable π - π intermolecular interactions.^{13b} In this paper, we will study how this architecture affects the second NLO activity.

Electrochemical, linear and NLO properties of systems in Chart 1 were carefully studied both experimental and theoretically and, eventually, compared to those of a planar conjugated analogue.

Results and discussion

Synthesis

Synthesis of compounds **1Ha,c**, **1Na,b** and **2a,c** is showed in Schemes 1, 2, 3 respectively, with the previously reported 4*H*-pyranylidene-containing aldehydes **1H-CHO**, **1N-CHO**, **2-CHO** (Chart 2)^{11d} as precursors.

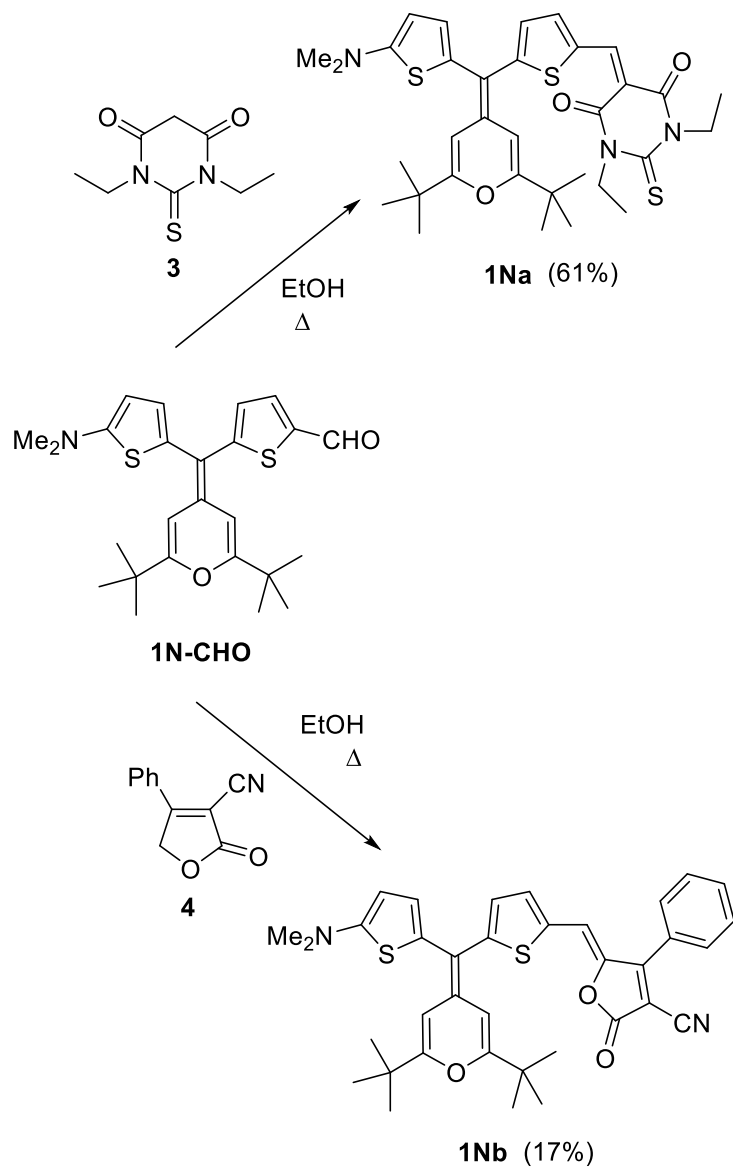


R: H **1H-CHO**

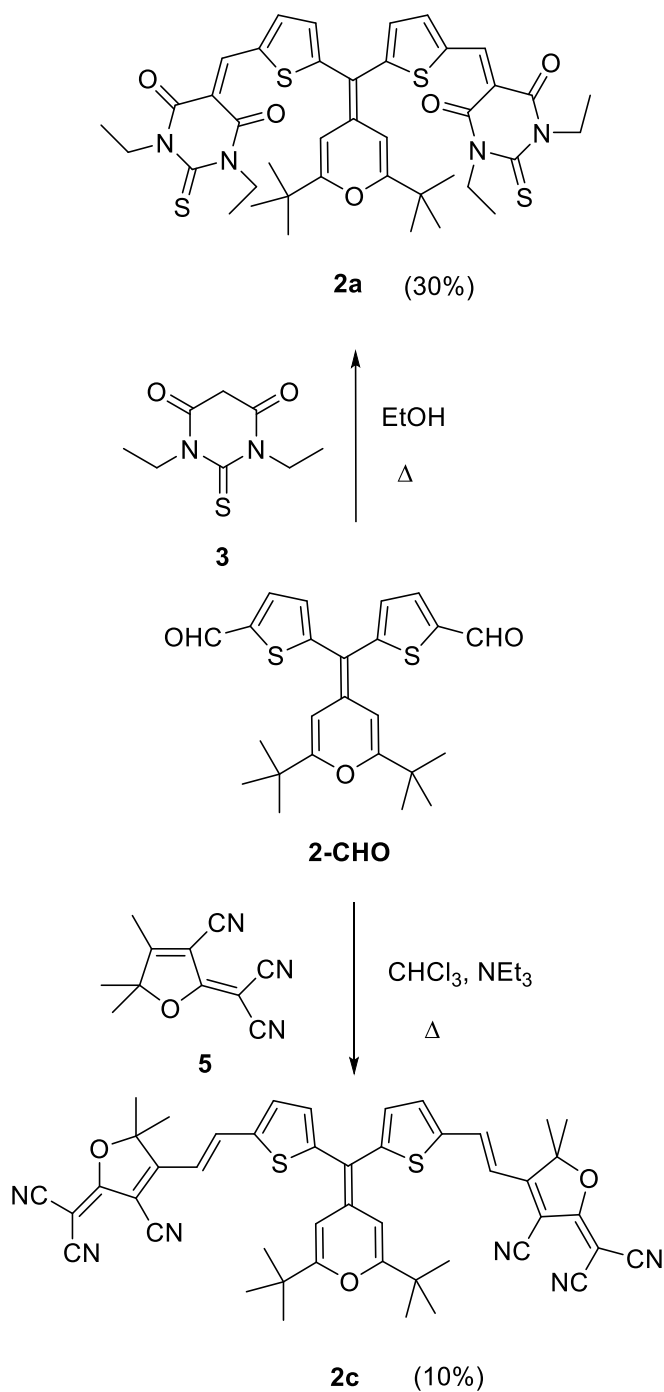
R: NMe₂ **1N-CHO**

R: CHO **2-CHO**

Chart 2. Precursor aldehydes. For their synthesis, see reference 11d.



Scheme 2: Preparation of 4H-pyranylidene-based push-pull molecules **1Na,b**.



Scheme 3: Synthesis of Y-shaped chromophores **2a,c**.

Chromophores were synthesized by Knoevenagel reaction between the aldehyde and the corresponding acceptors: (1,3-diethyl-2-thiobarbituric acid) (**3**), 4-phenyl-2-oxo-2,5-

dihydrofuran-3-carbonitrile (**4**)¹⁸ and 2-dicyanomethylene-3-cyano-4,5,5-trimethyl-2,5-dihydrofuran, TCF (**5**).¹⁹ The reaction conditions (base, solvent) have been adapted to the nature of the electron-withdrawing moiety.²⁰ Unfortunately, the TCF derivative **1Nc** could not be isolated.

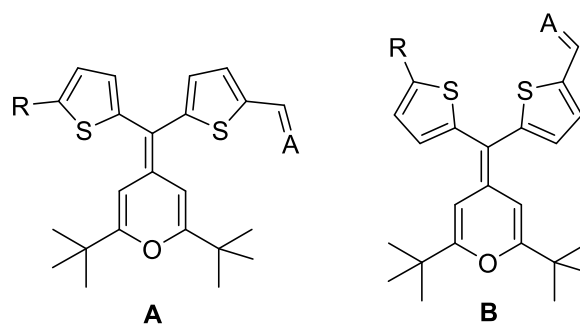
Purification of compounds **2a,c** required one step more compared to their analogues **1Ha,c** in order to separate traces of the mono-condensation products.

The new chromophores were characterized by IR, ¹H and ¹³C NMR spectroscopies and mass spectrometry (See Experimental Section). The analysis of the ³J_{HH} coupling constants allows us to infer that the CH=CH bond in compounds **c** has an *E* configuration.

Calculated Structures

The molecular geometry and electronic structure of the titled chromophores have been studied by means of DFT (Density Functional Theory) calculations. The CPCM (Conductor-like Polarizable Continuum Model) solvation method was used, choosing CH₂Cl₂ as solvent.

We have considered two possible conformations (**A** and **B** in Figure 1) for geometry optimizations.



R = H, NMe₂, CH=A
For A (acceptor): see Chart 1

Figure 1. Conformations used in geometry optimizations.

Calculations resulted in conformation **A** being more stable for compounds **1H** and **1Na**, while conformation **B** is more stable than **A** for compounds **2** and **1Nb**. Energy differences

between conformers were however below 1 kcal/mol with the exception of **1Hb** (4.89 kcal/mol) and **2b** (3.14 kcal/mol). Most molecular properties have been calculated using the most stable conformation, while NLO properties were calculated (See nonlinear optical properties section) on conformation **B**. The reason is that, since this has a larger dipole moment than **A**, it is expected to be favored by the large electric field used for the electric field-induced second harmonic generation (EFISHG) measurements.

The molecular geometry of these compounds results from the distortion caused by steric hindrance between pyrane and thiophene rings. For compounds **1H** and **1Na**, the thiophene spacer and the acceptor moiety are rotated approximately 15° with respect to the pyranilidene donor, thus allowing a good donor-acceptor conjugation. Contrary to this, the auxiliary donor thiophene ring is rotated by *ca.* 75° with respect to the pyrane ring and therefore does not interact with the donor-acceptor system (Figure S-26). This distortion from planarity is in accordance with that found in the related compounds recently reported as dyes for DSSC^{11d} or donor materials for OPV.^{13b}

Conformation **B** imposes a somewhat different geometry for **1Nb**, leading to a more distorted donor-thiophene-acceptor system with the thiophene spacer rotated 35° with respect to the pyranilidene unit, and the auxiliary thiophene donor rotated 57°.

Compounds **2**, having two identical acceptor groups, arrange in a C_2 symmetry with both thiophene rings rotated 40–45° with respect to the pyrane ring.

Bond lengths reflect the existence of two predominant resonance forms (Figure S-27): the neutral one and a zwitterionic form with the aromatized pyrylium donor and a quinoid thiophene spacer.

For compounds **1H** and **1N**, all the C–C bond lengths in the thiophene spacer equal to 1.39–1.40 Å, distance between the expected lengths for single and double C–C bonds, which reflects a similar contribution of both resonance forms. Contrary to this, the auxiliary thiophene shows clearly differentiated single (1.43 Å) and double (1.36–1.38 Å) C–C bonds.

The two acceptor chromophores **2**, having two equivalent thiophene rings, display a less marked quinoid character with single C–C bonds of 1.40–1.41 Å and double C=C bonds of 1.38–1.39 Å.

The contribution of these two resonance forms is also denoted by the natural bond orbital (NBO) charge analysis (Table 1 together with Figure 2 for notation of molecular domains). While the pyranilidene donor supports a positive charge ranging from +0.259 to +0.352, and the thiophene spacer and acceptor support an equivalent negative charge, the auxiliary thiophene donor (denoted as Th) in compounds **1H** and **1N** remains nearly uncharged (–0.007 to +0.002).

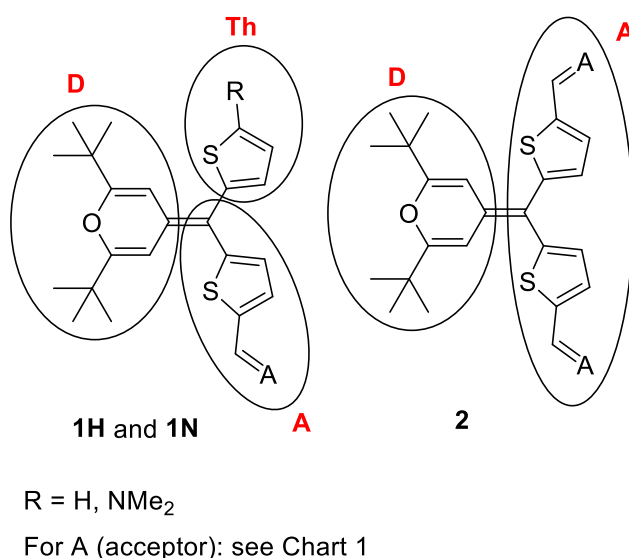


Figure 2. Molecular domains for title compounds.

Table 1. Calculated NBO charges (CPCM-M06-2x/6-31G*) in CH₂Cl₂ on different molecular domains (See Figure 2 for notation).

Compound	D	A	Th
1Ha	+0.352	-0.345	-0.007
1Na	+0.350	-0.350	0.000
2a	+0.351	-0.351	
1Hb	+0.299	-0.291	-0.008
1Nb	+0.259	-0.261	+0.002
2b	+0.296	-0.296	
1Hc	+0.339	-0.335	-0.004
2c	+0.338	-0.338	

Quite surprisingly, the charge on the pyrane ring of compounds **2** is nearly identical to that of their analogues **1H**, indicating that each acceptor group in **2** supports half the charge of their counterparts **1H**, and that the charge on the donor is related to the nature of the acceptor group rather than on the number of acceptors.

Electrochemical study

The electrochemical characterization of the chromophores has been performed by CV in CH₂Cl₂ solution using Bu₄NPF₆ as supporting electrolyte. Data are presented in Table 2, along with calculated HOMO and LUMO energies and first oxidation potentials, showing a fairly good agreement to experimental values. We included data for compound **6b**, analogue to **1Hb** lacking the thiophene unit, whose synthesis and comparative study is explained in NLO properties section.

Table 2: Electrochemical data^a and E_{ox} , E_{HOMO} and E_{LUMO} values theoretically calculated.^b

Compound	$E_{\text{ox1}}^{1/2}$ (V)	$E_{\text{ox2}}^{1/2}$ (V)	E_{red} (V)	$E_{\text{ox calc}}^c$ (V)	E_{HOMO} (eV)	E_{LUMO} (eV)
1Ha	0.71	1.00	-0.92	0.67	-6.42	-2.39
1Na	0.29 ^d		-1.01	0.19	-6.27	-2.37
2a	0.77	1.09	-1.00	0.75	-6.43	-2.43
1Hb	0.64 ^e	0.92 ^e	-0.87 ^e	0.54	-6.25 ^e	-2.56 ^e
1Nb	0.19	0.30	-0.91	0.13	-6.03	-2.50
2b	0.68 ^e	0.95 ^e	-0.82 ^e	0.63	-6.30 ^e	-2.58 ^e
1Hc	0.65	0.92	-0.73	0.63	-6.36	-2.71

2c	0.74	0.99	-0.70	0.77	-6.46	-2.77
6b^f	0.66	-	-0.92			

^a 5×10^{-4} M in CH₂Cl₂ versus Ag/AgCl (3 M KCl), glassy carbon working electrode, Pt counter electrode, 20 °C, 0.1 M NBu₄PF₆, 100 mV s⁻¹ scan rate. For these conditions: $E_{\text{ox}}^{1/2}$ ferrocene = +0.45 V. ^b Calculated at the CPCM-M06-2x/6-311+G(2d,p)//CPCM-M06-2x/6-31G* level in CH₂Cl₂. ^c Referenced to Ag/AgCl. ^d This wave corresponds to two oxidation processes. See interpretation in the text. ^e Data taken from ref. 13b. ^f See NLO section for synthesis and discussion of the properties.

All the voltammograms show three redox processes corresponding to one irreversible reduction peak (implicating the acceptor unit end) and two reversible oxidation steps, related to the two one-electron oxidations of the pyranilidene unit, as previously described for other chromophores with a similar design^{13b} and D- π -A platinum complexes with this donor end.²¹

There is a liaison between the structure of these systems and their electrochemical behavior, being the singular oxidation behavior of derivatives **1Na,b** the most remarkable.

The oxidation potentials values for **1Na,b** are extremely low for 4*H*-pyranilidene derivatives;^{9,10e} these compounds are easily oxidized, so the cation-radical and the dication generated are very stable species. The two oxidation waves for **1Na,b** are very close to each other, to the point of appearing practically together at 0.29 V with a "shoulder" in the case of **1Na** (Figure 3-top). Therefore, this compound was alternatively measured using a more sensitive electrochemical technique (Differential Pulse Voltammetry, DPV) which allowed the two expected oxidation peaks to be resolved (+0.25 V and +0.32 V respectively) (Figure 3-bottom). Precursor aldehyde **1N-CHO** (Chart 2) has a similar behavior, with two close oxidations processes at 0.19 and 0.34 V (no wave reduction was found).

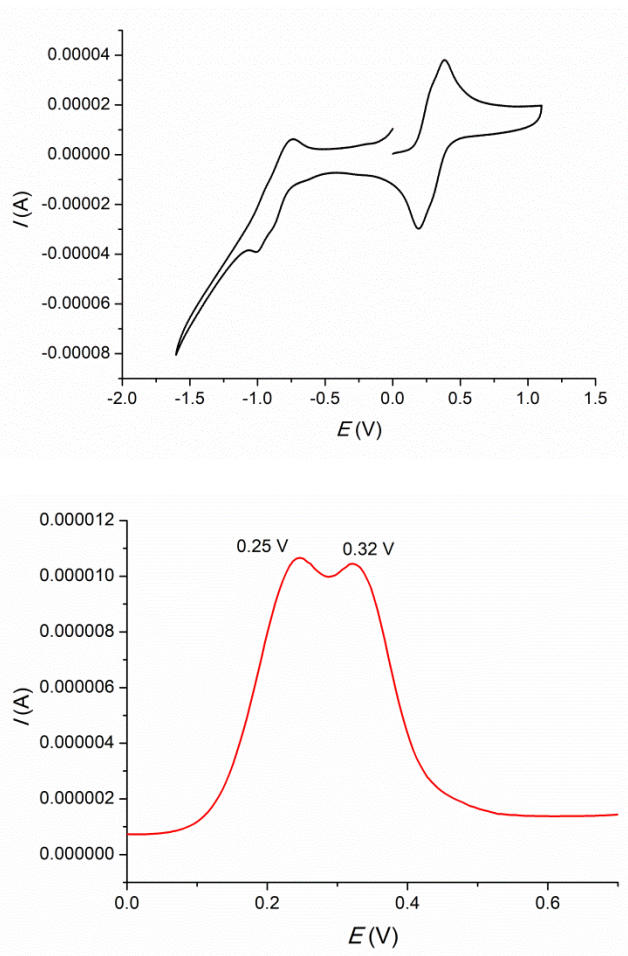


Figure 3: Voltammograms of compound **N1a**: CV (top) and DPV (bottom).

Hence, comparing compounds **1Na,b** with their analogues **1Ha,b** lacking the dimethylamino group, a considerable decrease of the oxidation half-potentials is observed, whereas the reduction potential is slightly increased; both facts agree with the presence of an excellent donor substituent. Evaluation of calculated E_{HOMO} (E_{LUMO}) data shows that systems **1N** have higher (only slightly higher) values than the corresponding **1H** analogues. Nevertheless, differences in HOMO energies are not large enough to rationalize the large decrease in oxidation potentials caused by the introduction of the dimethylamino group. We must consider that oxidation potentials arise from energy differences between the oxidized radical cations and neutral species and the large decrease in the oxidation potential caused by

the dimethylamino fragment is mainly due to the stabilization of the oxidized radical cation provided by this functional group.^{11d}

On the other hand, within each series (**1H**, **1N**, **2**), and focusing on the acceptor unit, $|E_{\text{red}}|$ decreases in the order **a** > **b** > **c**, corroborating the superior electron-withdrawing strength of the TCF unit, and points to a superior electron-withdrawing ability for furanone **4** than that could be expected. This trend is in agreement with computational calculations: E_{LUMO} decrease in the order **a** > **b** > **c**. Regarding E_{ox} values, both E_{ox1} and E_{ox2} decrease when passing from chromophores with the thiobarbiturate group (**a**) to their analogues **b,c**. In the case of Y-shaped compounds, system **2b** presents the lowest E_{ox} value.

Compounds **1H** and **1N**, with one acceptor moiety, show less anodic potentials than the corresponding analogues **2**; this result can be assigned to the higher planarization of the π -conjugated system in mono-functionalized compounds **1H** and **1N**, leading to an enhanced stabilization of the radical-cation.^{13b}

Eventually, the impact of this structural variation on $|E_{\text{red}}|$ values depends on the acceptor unit: for **a** series, with the thiobarbituric acid as electron withdrawing end, the lowest $|E_{\text{red}}|$ is found for compound **1Ha**, whereas for derivatives **b–c**, chromophores **2b** and **2c** show easier reduction processes.

Optical properties

UV–vis absorption data for the titled chromophores are gathered in Table 3. Different solvents with varied polarities have been used in the study. We included data for compound **6b**, analogue to **1Hb** lacking the thiophene unit, whose synthesis and comparative study is explained in NLO properties section.

Table 3: UV-vis absorption data.^a

Compound	λ_{abs} 1,4-dioxane	ϵ 1,4-dioxane	λ_{abs} CH ₂ Cl ₂	ϵ CH ₂ Cl ₂	λ_{abs} DMF	ϵ DMF
1Ha	611	43417	635	56896	620	40720
1Na	622	40453	646	41284	635	32790
2a	603	53816	627	56220	617	^b
1Hb	603	30205	645 ^c	38406 ^c	613	31197
1Nb	629	16410	671	14428	639	15062
2b	592	34628	626 ^c	40131 ^c	597	35355
1Hc	625	24569	707	31152	652	19163
2c	594	29464	664	31975	648	21224
6b^d			662	33940	645	30516

^a All λ_{abs} data in nanometer; the unit for ϵ is M⁻¹cm⁻¹. ^b Determination not possible due to the low solubility of the compound. ^c Data taken from ref. 13b. ^d See NLO section for synthesis and discussion of the properties.

Broad and intense bands located in the visible region can be observed for all compounds. These bands are related with an ICT process between the donor and the acceptor fragments. (Spectra are shown in Figures S-14 to S-23)

Concerning the presence of the dimethylamino group in the thiophene ring (comparison between compounds **1Ha-b** and **1Na-b**), a bathochromic shift of the ICT is encountered for systems **1N**. In contrast, the molar extinction coefficient (ϵ) decreases for the three solvents studied, being particularly important for furanone derivatives **b**, with a factor decrease of 2. Therefore, the dimethylamino substituent implies an absorption at higher wavelengths and a decrease in the ability to absorb the light.

As regards the effect of the acceptor end, it can be observed that variation of λ_{max} depends on the structure of the chromophore. For **1H** series, λ_{max} decreases in the order **c>b,a**. In the case of **1N** compounds, a red shift of the maximum absorption wavelength is observed for **1Nb** when compared to their analogue **1Na** for the three studied solvents. This feature

confirms, as it has been mentioned in the electrochemical study section, that furanone **4** could be read as an acceptor end stronger than thiobarbituric moiety.

In contrast, solvent is a factor to keep in mind for chromophores **2**: for the less polar 1,4-dioxane **2a** presents the highest λ_{\max} , while for the more polar DMF is the TCF derivative **2c** the compound with the largest λ_{\max} value. Moreover, thiobarbiturate systems **a** present larger ϵ values than their **b,c** counterparts, according to other Donor- π -thiobarbituric derivatives previously reported.⁹

The presence of one or two dimensional ICT, triggered by the presence of one or two acceptor units, has a significant influence on the electronic absorption properties of the studied systems. Thus, compounds **2** show blue-shifted absorptions and higher molar extinction coefficients when compared to their analogues **1H**. This latter feature is in agreement with previous results on other two dimensional chromophores including a *4H*-pyranylidene moiety.^{10d,22}

Data in Table 3 show for all compounds positive solvatochromism when comparing ~~on~~ 1,4-dioxane and CH₂Cl₂, which becomes negative on going from CH₂Cl₂ to DMF. This variety of behavior is the same found for other D- π -A compounds,²³ including some *4H*-pyranylidene derivatives.^{15,20a} A ground state with an enhanced contribution of the charge-separated resonance structure could be favored by increasing the polarity of the solvent^{23c} (CH₂Cl₂ to DMF), and could become greater than in the excited state giving rise to an hypsochromic effect.

The UV-Vis spectra of the new chromophores have been also studied using TD-DFT (Time Dependent DFT) calculations. The calculations were performed in dichloromethane using a CPCM (Conductor-like polarizable Continuum Model) solvation model and both **A** and **B** conformations (see Figure 1) were considered, since they are supposed to co-exist in solution at room temperature. These results are gathered in Table 4.

Table 4. TD-DFT calculated (CPCM-M06-2x/6-311+G(2d,p)//CPCM-M06-2x/6-31G*) absorption wavelengths and oscillator strengths (f) in dichloromethane.

Compound	Conformation A		Conformation B	
	λ (nm)	f	λ (nm)	f
1Ha	579	1.34	560	1.59
1Na	594	1.28	583	1.42
2a	575	1.68	553	0.66
	552	0.41	531	1.61
1Hb	623	1.20	610	1.71
1Nb	641	1.16	612	1.26
2b	611	1.69	571	0.64
	583	0.21	550	1.53
1Hc	651	1.58	616	1.82
2c	633	2.19	593	0.80
	595	0.26	563	1.96

The calculations underestimate the lower absorption wavelengths by 15–56 nm, denoting errors below 0.2 eV in excitation energies that are reasonable for this kind of calculations.²⁴ For compounds **1H** and **1N**, the excitation of a HOMO electron into the LUMO is the main contribution to the lowest energy transition. (see Figure 4).

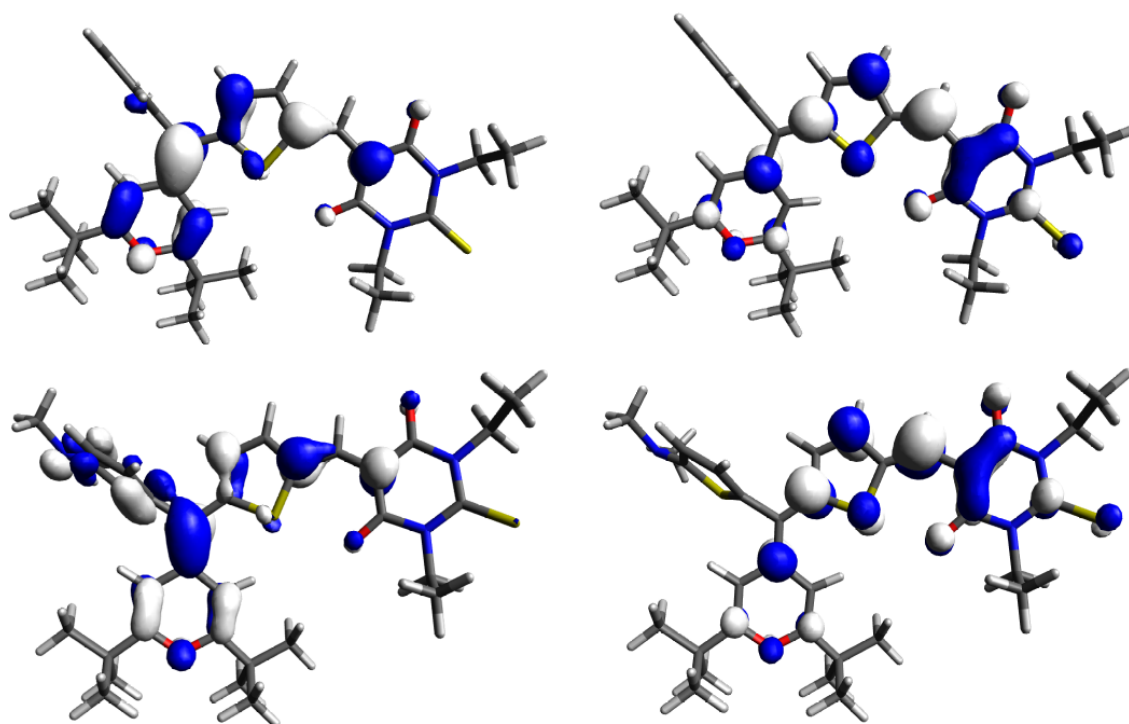


Figure 4. 0.04 contour plots of the HOMO (left) and LUMO (right) of compounds **1Ha** (top) and **1Na** (bottom).

Although the HOMO and LUMO are mainly located on the donor and on the acceptor, respectively, both frontier orbitals extend over the thiophene spacer. The large HOMO-LUMO overlap results in a large oscillator strength (f), and therefore a large ϵ .

Comparing **1H** and **1N** series, it can be seen (Figure 4) that the dimethylamino group increases the contribution of the auxiliary thiophene to the HOMO but not to the LUMO. The energy of the HOMO is therefore higher for compounds **1N** than for **1H** while the energy of LUMO is nearly identical, (see Table 2), thus a reduced HOMO-LUMO gap and consequently a bathochromic shift for **1N** with respect to **1H** is observed (see Table 3). Given that the auxiliary thiophene in compounds **1N** contributes to the HOMO but not to the LUMO, a reduced HOMO-LUMO overlap is encountered, causing lower f and ϵ values compared to **1H**.

Considering the effect of the acceptor group, its electron withdrawing strength causes a stabilization of the LUMO that results in lower HOMO-LUMO gaps and larger absorption wavelengths following this order $\mathbf{c} > \mathbf{b} > \mathbf{a}$, in agreement with experimental results.

The presence of two acceptor groups (compounds **2**) results in two unoccupied orbitals (LUMO and LUMO+1) (Figure 5) with similar energy arising from the combination of the orbitals of each acceptor moiety. This aspect provides two electronic transitions (HOMO \rightarrow LUMO and HOMO \rightarrow LUMO+1), close in energy, and probably overlap in the absorption spectrum resulting in large observed ϵ values.

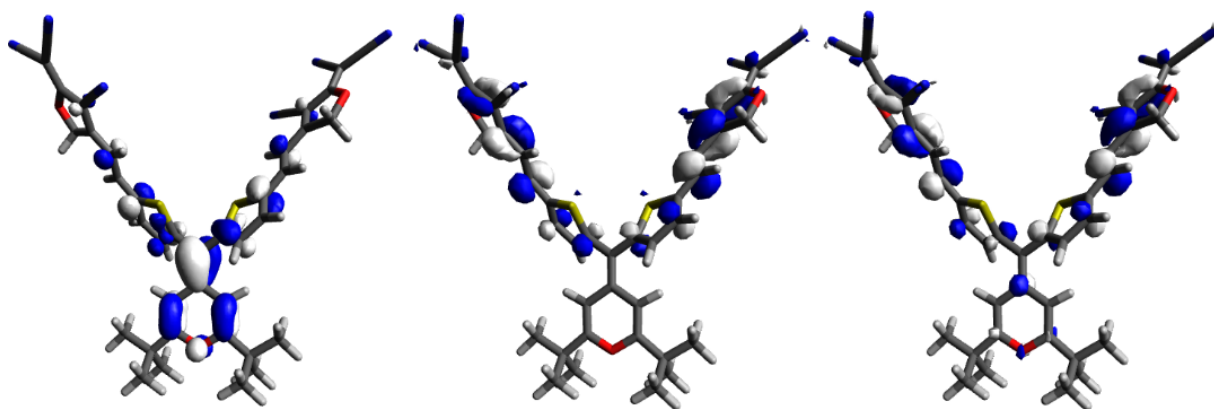


Figure 5. 0.04 contour plots of the HOMO (left), LUMO (center) and LUMO+1 (right) of compound **2c**.

For chromophores **1Na,b** bearing a dimethylamino group, the effect of its protonation in CH_2Cl_2 solution was studied by titration with trifluoroacetic acid (TFA) 10^{-2} M and registration of the corresponding absorption spectra. In order to have a good control of the titration process, compound **1Hb**, lacking the dimethylamino group was also studied. (Figure S-24).

In the case of compound **1Nb**, the changes observed in its UV-vis spectra upon the addition of this acid are illustrated in Figure 6.

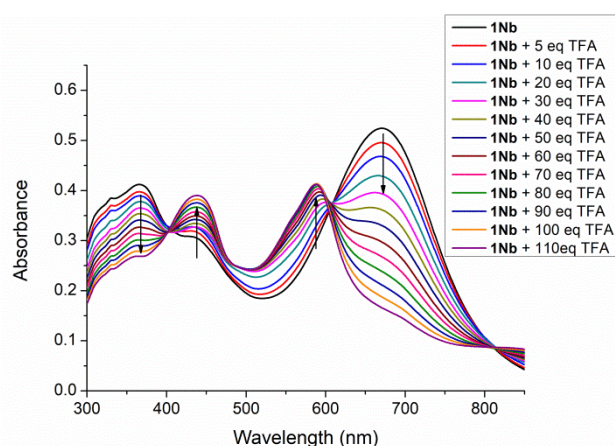


Figure 6. Absorption spectra of a CH_2Cl_2 solution of compound **1Nb** ($c = 3 \times 10^{-5}$ M) upon addition of TFA (5–110 eq.)

The progressive attenuation of the charge transfer absorption band for the neutral compound (centered at 671 nm) is encountered on increasing the concentration of acid, and a new higher-energy band corresponding to the protonated species appeared ($\lambda_{\text{max}} = 588$ nm). The difference of 83 nm accounts for the acceptor character of the protonated dimethylamino group.

On the other hand, the band in **1Nb** associated to transitions π - π^* (366 nm) decreases with protonation, with a new red-shifted band appearing (438 nm).

A significant TFA concentration (5 eq.) was needed before changes in the absorption spectra were remarked. Two isosbestic points were observed at 401 and 605 nm.

Comparing with the titration of compound **1Hb** (Figure S-24) the formation of other species apart the chromophore **1Hb** is not observed, validating the protonation of the dimethylamino group, with any sign of the protonation of other moieties in the chromophore.

Compound **1Na** (See Figure S-25) followed similar trends, although a sharper decrease of the ICT absorption was encountered and the disappearance of the band at 646 nm occurs with 40 equivalents of TFA.

Nonlinear Optical properties

In order to evaluate the second-order nonlinear response of the compounds, EFISHG measurements were performed at 1907 nm in dichloromethane. A simple two-level model²⁵ was used to obtain the dispersion corrected $\mu\beta_0$ values from the experimental $\mu\beta$. (Table 5) The second harmonic wavelength is not overlapped with any of the absorption bands of the studied compounds.

The benchmark chromophore Disperse Red 1 has been measured under the same experimental conditions. $\mu\beta_0$ values of 510×10^{-48} and 444×10^{-48} esu in CH_2Cl_2 and DMF respectively have been obtained.

Table 5. Experimental and calculated NLO properties.

Compound	$\mu\beta^a$ (10^{-48} esu)	$\mu\beta_0^b$ (10^{-48} esu)	$\mu\beta^c$ (10^{-48} esu)	$\mu\beta_0^d$ (10^{-48} esu)	μ^e (Debye)	β_0^e (10^{-30} esu)	$\mu\beta_0^e$ (10^{-48} esu)
1Ha	1260	625			12.0	78	841
1Na	1900	910			12.2	83	950
2a	1400	710			15.1	52	778
1Hb	2600	1250	1200	630	13.3	198	1795
1Nb	2050	910	1280	625	11.4	161	1278
2b	2350	1190	1050	575	13.4	139	1857
1Hc	5500	2140			21.5	211	4068
2c	3900	1770			30.4	140	4244
6b^f	2200	1000	1050	505			

^a $\mu\beta$ values determined in CH_2Cl_2 at 1907 nm (experimental uncertainty less than $\pm 15\%$). ^b

Experimental $\mu\beta_0$ values in CH_2Cl_2 extrapolated using the two-level model. ^c $\mu\beta$ values determined in DMF at 1907 nm (experimental uncertainty less than $\pm 20\%$). ^d Experimental $\mu\beta_0$ values in DMF calculated using the two-level model. ^e Calculated at the HF/6-31G*//CPCM-M06-2x/6-31G* level. ^f See below for synthesis and discussion of the properties.

Molecular hyperpolarizabilities (β) and dipole moments (μ) have also been estimated by quantum chemical calculations. Having in mind that DFT methods usually fail to determine nonlinear optical properties,²⁶ calculations have been performed using the HF (Hartree-Fock) method. While theoretical results overestimate the experimental values, they reproduce the observed trends.

With respect to the influence of the electron-withdrawing end on the NLO properties of the studied chromophores, for series **1H** and **2**, the nonlinearities increase in the order $\mathbf{a} < \mathbf{b} < \mathbf{c}$, which again indicates the higher acceptor ability of the TCF unit. Modification of the acceptor is more significant for **1H** systems than for Y-chromophores **2**. The increasing trend when acceptor changes from **a** to **c** is also reproduced by theoretical calculations. Considering a two level approach,^{25a,27} hyperpolarizability depends on the transition dipole moment (μ_{01}) or the oscillator strength (f), the dipole moment change on excitation ($\Delta\mu_{01}$) and the excitation energy (E_{01}). The change in the molecular hyperpolarizability may be mostly due to the decreased excitation energies along the series $\mathbf{a} > \mathbf{b} > \mathbf{c}$.

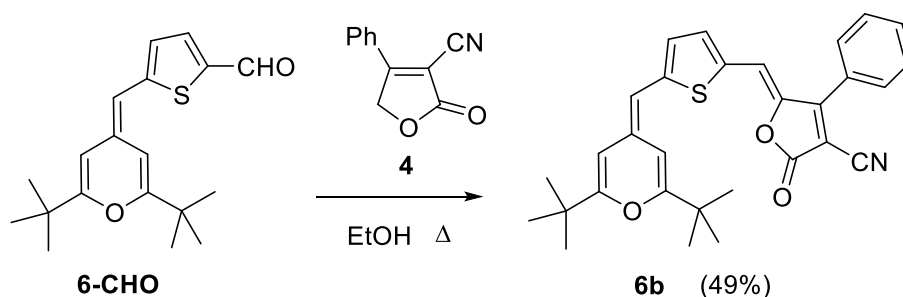
On the other hand, compounds **1Na-b** show essentially the same NLO response. Theoretical calculations show that while the hyperpolarizability (β_0) of **1Nb** is more than double that of **1Na**, the dipole moment is better aligned to the β_0 vector in **1Na** (22°) than in **1Nb** (46°), thus resulting in scarce differences in the dot product $\mu\beta_0$.

The effect of the dimethylamino group in the NLO properties depends on the acceptor unit. Thus, for thiobarbituric derivatives **a**, going from **1H** chromophore to **1N** one implies an increase on the NLO response, ($\mu\beta_0$ (**1Na**)/ $\mu\beta_0$ (**1Ha**) = 1.46). Nonetheless, for furanone derivatives **b**, a slight decrease in the $\mu\beta_0$ value is observed ($\mu\beta_0$ (**1Nb**)/ $\mu\beta_0$ (**1Hb**) = 0.73).

Theoretical calculations also show that the effect of the dimethylamino fragment on hyperpolarizability depends on the acceptor. Paying attention to the parameters involved in the two level approach, this substituent causes a decreased excitation energy (E_{01}) accompanied by a decreased oscillator strength (f) and an increased dipole moment change ($\Delta\mu_{01}$). The relative weight to these opposed factors determines the final increased or decreased hyperpolarizability.

Y-compounds **2** (except **2a** with a thiobarbituric acid acceptor) show lower experimental $\mu\beta_0$ values than those of their analogues **1H**. This result can be considered a bit surprising since the opposite trend has been observed in other chromophores with the pyran ring incorporated into the π -spacer,^{22a-b,28} acting as donor in D-A-D compounds^{10a,d} or in A-D-A systems.^{21c} While theoretical calculations do not reproduce exactly the trends in $\mu\beta_0$ values on passing from compounds **1H** to **2**, the calculated values for chromophores **2** are similar to their **1H** analogues. The calculations reveal that the effect of the increased dipole moment on passing from **1H** to **2** is opposed by a decreased hyperpolarizability, and therefore the resulting $\mu\beta_0$ depends on the relative effect of these parameters.

In order to study the effect of the additional thiophene ring, nearly orthogonal to the extended π -system, on the final properties, compound **6b**, analogue to derivative **1Hb** lacking this unit, was prepared (Scheme 4). This compound was synthesized from the previously reported aldehyde **6-CHO**²⁹ and acceptor **4**. The electrochemical and optical properties of this new chromophore are gathered in Tables 2, 3 and 5.



Scheme 4: Synthesis of compound **6b**.

Comparison of compounds **1Hb** and **6b** shows that **6b**, lacking the thiophene ring, features (i) a red shift in λ_{abs} ^{13b} together with a decrease for the ϵ value^{13b}; (ii) a single irreversible anodic peak corresponding to the formation of the pyrylium radical cation and subsequent dimerization process, as described for other methylene pyran derivatives³⁰ together with a

slightly more cathodic E_{red} value; (iii) a decrease in the NLO response. Hence, it is noteworthy that chromophore **1Hb**, with the auxiliary thiophene ring while being more transparent shows a higher NLO activity ($\mu\beta_0$ (**1Hb**)/ $\mu\beta_0$ (**6b**) = 1.25).

Calculations on **6b** predict a bathochromic shift with respect to **1Hb** (635 nm vs 623 nm on the more stable conformation **A**), but a nearly identical NLO behaviour with $\mu\beta_0 = 1794 \times 10^{-48}$ esu (on the more polar conformation **B**).

In order to study the influence of solvent in the NLO activity, measurements in DMF were performed for furanone-containing derivatives **b**. These measurements show some limitations: it is not a usual solvent and its EFISH parameters are not accurately calibrated. For these reasons, $\mu\beta$ values (10^{-48} esu) given in table 5 present a wider margin of error (20%), although the reproducibility is similar to that observed in CH_2Cl_2 .

The lower $\mu\beta_0$ values obtained in DMF indicate that **b** chromophores are more polarized in this solvent than in dichloromethane, (the zwitterionic form of Figure S-27 has a more important presence than in CH_2Cl_2) and that these systems are left-handed chromophores in Marder's plot³¹ (A/B region), with the neutral form predominating in this solvent polarity range.

Conclusion

Three series of compounds featuring a 4*H*-pyranilydene moiety have been designed and studied, based on two current approaches for the optimization of NLO properties: twisted chromophores (series **1H** and **1N**) and multidimensional charge transfer (series **2**).

Y-arranged chromophores **2** show lower absorption wavelengths, higher E_{ox} values and lower $\mu\beta_0$ values than their one-dimensional analogues **1H**. Thiobarbituric acid derivatives represent an exception to the trend observed in NLO response.

The incorporation of 5-dimethylaminothiophene moiety in the exocyclic C=C bond of the pyranilidene unit leads to derivatives **1N** to be easily oxidized. The effect of this non coplanar moiety in the NLO response depends on the acceptor unit.

Twisted chromophore **1Hb**, with the thiophene ring in the exocyclic position, show higher NLO activity and wider transparency range than the analogue **6b**, lacking this moiety. These results point out that this design is suitable to achieve structures with high second-order NLO responses, allowing an isolating effect needed for preparing organic electro-optic devices.

Experimental section

General experimental methods

Infrared measurements were carried out in KBr using a Fourier Transform Infrared spectrometer. Melting points were obtained in open capillaries and are uncorrected. ¹H-NMR spectra were recorded at 300 or 400 MHz. ¹³C-NMR spectra were recorded at 100 MHz respectively; δ values are given in ppm (relative to TMS) and *J* values in Hz. The apparent resonance multiplicity is described as s (singlet), d (doublet), t (triplet), q (quartet) and m (multiplet). Electrospray mass spectra were recorded on a Bruker Q-ToF spectrometer; accurate mass measurements were achieved using sodium formate as external reference.

Cyclic Voltammetry measurements were performed using a glassy carbon working electrode, Pt counter electrode, and Ag/AgCl reference electrode. The experiments were carried out under argon in CH₂Cl₂, with Bu₄NPF₆ as supporting electrolyte (0.1 mol L⁻¹). Step potential was 0.01 V and the interval time 0.5 s.

Electric field induced second harmonic generation (EFISH) measurements have been carried out using an excitation wavelength of 1907 nm. This fundamental radiation is the output of a H₂ Raman shifter pumped by a Q-switched Nd:YAG laser at 1064 nm. The laser repetition rate is 10 Hz and the pulse width 8 ns. A computer controlled NLO spectrometer

completes the SHG experimental set-up. The excitation beam is split in two; the less intense one is directed to a *N*-(4-nitrophenyl)-(*L*)-prolinol (NPP) powder sample whose SH signal is used as a reference in order to reduce the effects of laser fluctuations. The second one is passed through a linear (vertical) polarizer and focused into the EFISH wedge shaped liquid cell. Voltage pulses of 5 kV and 3 μ s are applied across the cell (2 mm gap between the electrodes) synchronously with the laser pulses. The harmonic signals from both the EFISH cell and the NPP reference are measured with two photomultipliers. Interference filters are used to remove the residual excitation light beyond the sample and the reference.

The molecular $\mu\beta$ values of the reported compounds have been determined in dichloromethane and DMF (for **b** derivatives). Several solutions of concentration in the range 1.5×10^{-3} – 5×10^{-4} M were measured. $\mu\beta_0$ values were extrapolated using a two-level dispersion model^{25a} and λ_{\max} corresponding to the lowest energy band. Under the same experimental conditions $\mu\beta_0$ deduced for DR1 in dichloromethane was 510×10^{-48} esu, quite close to the value reported in the same solvent by Dirk et al.³² For DMF, the deduced value was 444×10^{-48} esu.

Density Functional Theory (DFT) calculations were performed using Gaussian 16³³ with the ultrafine integration grid. Solvent effects were estimated using a Conductor-like Polarizable Continuum Model (CPCM).^{34,35} Equilibrium geometries were optimized using the M06-2x hybrid meta-GGA exchange correlation functional³⁶ and the medium size 6-31G* base.³⁷ Optimized geometries were characterized as minima by frequency calculations. Excitation energies were calculated by time-dependent single point calculations using the M06-2x/6-311G (2d,p) model chemistry. Absorption spectra were estimated through the calculation of vertical excitations at the ground state geometry. Ground state oxidation potentials (E_{ox}) were calculated using the M06-2x/6-311-G (2d,p) energies and calculating the

thermal corrections to Gibbs free energy at the M06-2x/6-31G* level. Molecular Orbital contour plots were obtained using the Avogadro software³⁸ at 0.04 isosurface value.

Aldehydes **1H-CHO**,^{11d} **1N-CHO**,^{11d} **2-CHO**^{11d} and **6-CHO**²⁹ and acceptors **4**¹⁸ and **5**¹⁹ were prepared as previously described.

5-((5-((2,6-di-*tert*-butyl-4*H*-pyran-4-ylidene)(thiophen-2-yl)methyl)thiophen-2-yl)methylene-1,3-diethyl-2-tioxodihydropyrimidine-4,6(1*H*,5*H*)-dione (1Ha)

A mixture of aldehyde **1H-CHO** (50 mg, 0.125 mmol) and 1,3-diethyl-2-thiobarbituric acid (**3**) (28 mg, 0.14 mmol) in absolute ethanol (3 mL) was refluxed in a heating block under argon with exclusion of light for 7 hours (TLC monitoring). After cooling, the resulting solid was isolated by filtration and washed with cold pentane. A green solid was obtained (51.6 mg; 71 %).

Mp (°C) 226–228. IR (KBr): ν (cm⁻¹) 2973 (Csp³-H), 1647 (C=O), 1551, 1530 and 1501 (C=C Ar.), 1393 (C=S). ¹H NMR (CD₂Cl₂, 300 MHz): δ 8.48 (s, 1H), 7.73 (d, *J* = 4.5 Hz, 1H), 7.41 (dd, *J*₁ = 5.2 Hz, *J*₂ = 1.2 Hz, 1H), 7.13–7.10 (m, 2H), 6.95–6.93 (m, 2H), 5.92 (d, *J* = 2.2 Hz, 1H), 4.57–4.49 (m, 4H), 1.31 (s, 9H), 1.28–1.22 (m, 6H), 1.13 (s, 9H). ¹³C {¹H} NMR (CD₂Cl₂, 100 MHz): δ 179.4, 168.9, 167.5, 165.8, 161.9, 160.4, 148.0, 147.2, 142.8, 138.9, 135.1, 129.0, 128.3, 127.9, 126.9, 108.8, 107.7, 104.4, 102.9, 44.1, 43.4, 36.8, 36.4, 28.2, 28.1, 12.7. HRMS (ESI⁺/Q-TOF) *m/z*: [M]⁺ Calcd for C₃₁H₃₆N₂O₃S₃ 580.1883; Found 580.1862.

(*E*)-2-(3-cyano-4-(2-(5-((2,6-di-*tert*-butyl-4*H*-pyran-4-ylidene)(thiophen-2-yl)methyl)thiophen-2-yl)vinyl)-5,5-dimethylfuran-2(5*H*)-yliden)malononitrile (1Hc)

Triethylamine (41 μ L, 0.30 mmol) was added to a solution of **1H-CHO** (119.4 mg, 0.30 mmol) and acceptor TCF (**5**; 66.3 mg, 0.33 mmol) in CHCl₃ (6 mL) under an argon atmosphere, and the mixture was refluxed in a heating block for 5 days. (TLC monitoring)

Then, the solvent was evaporated and the crude product was purified by flash chromatography (silica gel), using hexane/AcOEt 8:2 as eluent to afford a dark blue solid (26 mg; 15 %).

Mp (°C) 278–279 (dec.). IR (KBr): ν (cm⁻¹) 2926 (Csp³-H), 2219 (C≡N), 1658 (C=C), 1595, 1558 and 1533 (C=C Ar.).

¹H NMR (CD₂Cl₂, 400 MHz): δ 7.78 (d, J = 15.5 Hz, 1H), 7.42–7.41 (m, 2H), 7.10 (dd, J_1 = 5.2 Hz, J_2 = 3.5 Hz, 1H), 6.97 (d, J = 4.4 Hz, 1H), 6.94 (dd, J_1 = 3.5 Hz, J_2 = 1.2 Hz, 1H), 6.75 (d, J = 2.1 Hz, 1H), 6.48 (d, J = 15.5 Hz, 1H), 5.91 (d, J = 2.1 Hz, 1H), 1.71 (s, 6H), 1.28 (s, 9H), 1.14 (s, 9H). ¹³C{¹H} NMR (CD₂Cl₂, 100 MHz): δ 173.7, 168.1, 166.9, 158.0, 143.3, 140.0, 137.8, 137.5, 137.1, 128.9, 127.9, 126.8, 113.2, 112.6, 112.0, 111.2, 107.9, 103.7, 101.9, 97.6, 67.1, 36.6, 36.3, 28.2, 28.1, 26.9. HRMS (ESI⁺/Q-TOF) m/z [M+Na]⁺ Calcd for C₃₄H₃₃N₃NaO₂S₂ 602.1906; Found 602.1932.

**5-5'-((((2,6-di-*tert*-butyl-4*H*-pyran-4-ylidene)methylene)bis(thiophene-2,5-diyl))bis(methanylylidene))bis(1,3-diethyl-2-thioxodihydropyrimidine-4,6(1*H*,5*H*)-dione)
(2a)**

A mixture of aldehyde **2-CHO** (80 mg, 0.19 mmol) and 1,3-diethyl-2-thiobarbituric acid (**3**) (80 mg; 0.40 mmol) in absolute ethanol (5 mL) was refluxed in a heating block under argon with exclusion of light for 24 hours (TLC monitoring). After cooling, the resulting solid was isolated by filtration, washed with cold pentane, and finally purified by flash chromatography (silica gel) with CH₂Cl₂ as eluent. A dark blue solid was obtained (47 mg; 30 %).

Mp (°C) 290–291 (dec.). IR (KBr): ν (cm⁻¹) 3072 (Csp²-H), 2980 (Csp³-H), 1684 (C=O), 1655 (C=C), 1547 and 1515 (C=C Ar.), 1395 (C=S). ¹H NMR (CD₂Cl₂, 400 MHz): δ 8.62 (s, 2H), 7.88 (d, J = 4.2 Hz, 2H), 7.13 (d, J = 4.2 Hz, 2H), 6.62 (s, 2H), 4.58–4.51 (m, 8H), 1.30–1.25 (m, 30H). ¹³C{¹H} NMR (CD₂Cl₂, 100 MHz): δ 179.4, 169.1, 162.8, 161.6, 160.3, 148.9, 147.2, 139.7, 136.9, 129.9, 109.9, 108.1, 103.8, 44.3, 43.6, 36.7, 30.3, 28.1, 12.7. HRMS (ESI⁺/Q-TOF) m/z : [M+Na]⁺ Calcd for C₄₀H₄₆N₄NaO₅S₄ 813.2243; Found 813.2228.

(*E,E*)-2,2'-(((2,6-di-*tert*-butyl-4*H*-pyran-4-ylidene)methylene)bis(thiophene-2,5-diyl))bis(ethene-1,2-diyl))bis(3-cyano-5,5-dimethylfuran-4(*5H*)-yl-2(*5H*-ylidene))dimalononitrile (2c)

Triethylamine (68 μ L, 0.50 mmol) was added to a solution of **2-CHO** (80 mg, 0.19 mmol) and acceptor TCF (**5**; 100 mg, 0.50 mmol) in CHCl_3 (6 mL) under an argon atmosphere, and the mixture was refluxed in a heating block for 3 days (TLC monitoring). Then, the solvent was evaporated and the crude product was purified by flash chromatography (silica gel), using hexane/AcOEt 8:2 as eluent. A further purification by flash chromatography (silica gel) with $\text{CH}_2\text{Cl}_2/\text{AcOEt}$ 9.7:0.3 was needed. Finally, the resulting solid was washed with cold pentane to afford compound **2c** as a dark blue solid. (15 mg; 10%)

Mp ($^{\circ}\text{C}$) 172–173. IR (KBr): ν (cm^{-1}) 2963 ($\text{Csp}^3\text{-H}$), 2224 ($\text{C}\equiv\text{N}$), 1659 ($\text{C}=\text{C}$), 1577 ($\text{C}=\text{C}$ Ar.). ^1H NMR (CD_2Cl_2 , 400 MHz): δ 7.72 (d, $J = 15.8$ Hz, 2H), 7.45 (d, $J = 4.0$ Hz, 2H), 7.04 (d, $J = 4.0$ Hz, 2H), 6.60 (d, $J = 15.8$ Hz, 2H), 6.39 (s, 2H), 1.75 (s, 12H), 1.22 (s, 18H). $^{13}\text{C}\{^1\text{H}\}$ NMR (CD_2Cl_2 , 100 MHz): δ 173.9, 168.5, 154.4, 139.7, 139.6, 138.2, 137.0, 130.0, 113.0, 112.8, 112.2, 111.5, 102.9, 97.9, 36.6, 31.2, 28.1, 26.9. HRMS (ESI⁺/Q-TOF) m/z : $[\text{M}+\text{Na}]^+$ Calcd for $\text{C}_{46}\text{H}_{40}\text{N}_6\text{NaO}_3\text{S}_2$ 811.2496; Found 811.2470.

5-(((5-((2,6-di-*tert*-butyl-4*H*-pyran-4-ylidene)(5-(dimethylamino)thiophen-2-yl)methyl)thiophen-2-yl)methylene)-1,3-diethyl-2-thioxodihydropyrimidine-4,6(1*H*, 5*H*)-dione (1Na)

This compound was prepared by following the same procedure as for **1Ha**, starting from **1N-CHO** (54 mg, 0.12 mmol) with a reaction time of 5 h. A dark blue solid was obtained (47 mg; 61 %).

Mp ($^{\circ}\text{C}$) 176–180. IR (KBr): ν (cm^{-1}) 2965 and 2868 ($\text{Csp}^3\text{-H}$), 1653 ($\text{C}=\text{O}$), 1537 ($\text{C}=\text{C}$, Ar.), 1382 ($\text{C}=\text{S}$). ^1H NMR (CD_2Cl_2 , 400 MHz): δ 8.49 (s, 1H), 7.78 (d, $J = 4.4$ Hz, 1H), 7.12 (d, $J = 4.4$ Hz, 1H), 6.98 (d, $J = 2.1$ Hz, 1H), 6.62 (d, $J = 3.7$ Hz, 1H), 6.17 (d, $J = 2.1$ Hz,

1H), 5.85 (d, $J = 3.7$ Hz, 1H), 4.58–4.52 (m, 4H), 2.93 (s, 6H), 1.30–1.25 (m, 15H), 1.19 (s, 9 H). $^{13}\text{C}\{^1\text{H}\}$ NMR (CD_2Cl_2 , 100 MHz): δ 179.4, 167.4, 161.9, 160.4, 147.9, 147.5, 135.3, 129.1, 128.2, 126.5, 44.1, 43.4, 31.2, 28.2, 12.8. HRMS (ESI⁺/Q-TOF) m/z $[\text{M}]^+$ Calcd for $\text{C}_{33}\text{H}_{41}\text{N}_3\text{O}_3\text{S}_3$; 623.2305; Found 623.2315; m/z $[\text{M}+\text{Na}]^+$ Calcd for $\text{C}_{33}\text{H}_{41}\text{N}_3\text{NaO}_3\text{S}_3$ 646.2202; Found 646.2184.

5-((5-((2,6-di-*tert*-butyl-4*H*-pyran-4-ylidene)methyl)thiophen-2-yl)methylene)-2-oxo-4-phenyl-2,5-dihydrofuran-3-carbonitrile (1Nb)

To a solution of aldehyde **1N-CHO** (66 mg, 0.15 mmol) in absolute ethanol (4 mL) acceptor **4** (30.5 mg; 0.16 mmol) was added. The mixture was refluxed in a heating block under argon with exclusion of light for 48 hours (TLC monitoring). After cooling, the resulting solid was isolated by filtration and washed with cold pentane. Finally, filtration through a plug of silica gel with hexane/AcOEt 9.8:0.2 as eluent afforded a dark green solid (16 mg, 17 %).

Mp ($^\circ\text{C}$) 217–219. IR (KBr): ν (cm^{-1}) 2923 ($\text{Csp}^3\text{-H}$), 2224 ($\text{C}\equiv\text{N}$), 1749 ($\text{C}=\text{O}$), 1659 ($\text{C}=\text{C}$), 1604 and 1543 ($\text{C}=\text{C}$, Ar.). ^1H NMR (CD_2Cl_2 , 400 MHz): δ 7.64–7.59 (m, 5H), 7.42 (d, $J = 4.3$ Hz, 1H), 7.02 (d, $J = 4.3$ Hz, 1H), 6.73 (s, 1H), 6.62 (d, $J = 2.1$ Hz, 1H), 6.61 (d, $J = 3.8$ Hz, 1H), 6.12 (d, $J = 2.1$ Hz, 1H), 5.81 (d, $J = 3.8$ Hz, 1H), 2.92 (s, 6H), 1.24 (s, 9H), 1.17 (s, 9H). $^{13}\text{C}\{^1\text{H}\}$ NMR: not registered due to its low solubility. HRMS (ESI⁺/Q-TOF) m/z : $[\text{M}]^+$ Calcd for $\text{C}_{36}\text{H}_{36}\text{N}_2\text{O}_3\text{S}_2$ 608.2162; Found 608.2169.

5-((5-((2,6-di-*tert*-butyl-4*H*-pyran-4-ylidene)methyl)thiophen-2-yl)methylene)-2-oxo-4-phenyl-2,5-dihydrofuran-3-carbonitrile (6b)

A solution of aldehyde **6-CHO** (173.3 mg, 0.55 mmol) and acceptor **4** (104.3 mg, 0.56 mmol) in EtOH (10 mL) was refluxed in a heating block for 24 h under an argon atmosphere

(TLC monitoring), then the solvent was evaporated under reduced pressure. The crude was purified by flash chromatography (silica gel) using hexane/AcOEt 9:1 as eluent to obtain a blue solid. (131.3 mg, 49%).

Mp (°C) 79 (dec.). IR (KBr): ν (cm⁻¹) 3062 (Csp²-H), 2964 (Csp³-H), 2219 (C≡N), 1751 (C=O), 1659, 1601 and 1538 (C=C, Ar.). ¹H NMR (CD₂Cl₂, 400 MHz): δ 7.64–7.61 (m, 5 H), 7.45 (d, *J* = 4.3 Hz, 1 H), 6.91 (d, *J* = 4.3 Hz, 1 H), 6.76 (s, 1 H), 6.61 (d, *J* = 1.9 Hz, 1 H), 5.98 (s, 1 H), 5.88 (d, *J* = 1.9 Hz, 1 H), 1.32 (s, 9 H), 1.24 (s, 9 H). ¹³C{¹H} NMR (CD₂Cl₂, 100 MHz): δ 167.5, 164.7, 164.3, 159.6, 154.7, 141.4, 136.4, 134.8, 132.0, 131.2, 128.9, 128.4, 127.9, 126.0, 115.1, 112.6, 105.3, 104.5, 100.0, 35.7, 35.1, 27.2 (×2). HRMS (ESI⁺/Q-TOF) *m/z*: [M+Na]⁺ Calcd for C₃₀H₂₉NNaO₃S 506.1760; Found 506.1761.

Supporting Information. The Supporting Information is available free of charge at...

General experimental methods, NMR and UV–vis spectra of new compounds, NLO measurements and computed energies and Cartesian coordinates of optimized geometries of all chromophores.

Acknowledgments. Financial support from Ministerio de Ciencia e Innovación (PID2019-104307GB-I00/AEI/10.13039/501100011033), Gobierno de Aragón-FEDER-Fondo Social Europeo 2014–2020 (E14_17R) and University of Zaragoza (UZ2019-CIE-01) is gratefully acknowledged.

References

[1] a) Dalton, L. R.; Sullivan, P. A.; Bale, D. H. Electric Field Poled Organic Electro-optic Materials: State of the Art and Future Prospects. *Chem. Rev.* **2010**, *110*, 25–55; b) Stegeman,

- G. I.; Stegeman R. A. in *Nonlinear Optics: Phenomena, Materials, and Devices*, (Ed.: Boreman, G.), Wiley Series in Pure and Applied Optics, John Wiley & Sons: Hoboken, 2012.
- [2] Garmire, E. Nonlinear optics in daily life. *Opt. Express* **2013**, *21*, 30532–30544.
- [3] Dalton, L. R.; Günter, P.; Jazbinsek, M.; Kwon, O.P.; Sullivan, P.A. *Organic Electro-Optics and Photonics: Molecules, Polymers and Crystals*, Cambridge Univ. Press, UK, 2015.
- [4] Liu, J.; Ouyang, C.; Huo, F.; He, W.; Cao, A. Progress in the enhancement of electro-optic coefficients and orientation stability for organic second-order nonlinear optical materials. *Dyes Pigm.* **2020**, *181*, 108509.
- [5] Bureš, F. Fundamental aspects of property tuning in push–pull molecules. *RSC Adv.* **2014**, *4*, 58826–58851, and references cited therein.
- [6] Li, M.; Li, Y.; Zhang, H.; Wang, S.; Ao, Y.; Cui, Z. Molecular engineering of organic chromophores and polymers for enhanced bulk second-order optical nonlinearity. *J. Mater. Chem. C* **2017**, *5*, 4111–4122.
- [7] Klikar, M.; Solanke, P.; Tydlitát, J.; Bureš, F. Alphabet-Inspired Design of (Hetero)Aromatic Push–Pull Chromophores. *Chem. Rec.* **2016**, *16*, 1886–1905, and references cited therein.
- [8] a) Shi, Y.; Frattarelli, D.; Watanabe, N.; Facchetti, A.; Cariati, E.; Righetto, S.; Tordin, E.; Zuccaccia, C.; Macchioni, A.; Wegener, S. L.; Stern, C. L.; Ratner M. A.; Marks, T. J. Ultra-High-Response, Multiply Twisted Electro-optic Chromophores: Influence of π -System Elongation and Interplanar Torsion on Hyperpolarizability. *J. Am. Chem. Soc.* **2015**, *137*, 12521–12538; b) Lou, A. J.-T.; Righetto, S.; Cariati, E.; Marks, T. J. Organic Salts Suppress Aggregation and Enhance the Hyperpolarizability of a π -Twisted Chromophore. *Chem. Eur. J.* **2018**, *24*, 15801–15805.

[9] Andreu, R.; Carrasquer, L.; Franco, S.; Garín, J.; Orduna, J.; Martínez de Baroja, N.; Alicante, R.; Villacampa, B.; Allain, M. 4*H*-Pyran-4-ylidenes: Strong Proaromatic Donors for Organic Nonlinear Optical Chromophores. *J. Org. Chem.* **2009**, *74*, 6647–6657.

[10] Selected examples: a) Andreu, R.; Galán, E.; Garín, J.; Herrero, V.; Lacarra, E.; Orduna, J.; Alicante, R.; Villacampa, B. Linear and V-Shaped Nonlinear Optical Chromophores with Multiple 4*H*-Pyran-4-ylidene Moieties. *J. Org. Chem.* **2010**, *75*, 1684–1692. b) Andreu, R.; Galán, E.; Orduna, J.; Villacampa, B.; Alicante, R.; López Navarrete, J. T.; Casado, J.; Garín, J. Aromatic/Proaromatic Donors in 2-Dicyanomethylenethiazole Merocyanines: From Neutral to Strongly Zwitterionic Nonlinear Optical Chromophores. *Chem. Eur. J.* **2011**, *17*, 826–838; c) Poronik, Y. M.; Hugues, V.; Blanchard-Desce, M.; Gryko, D. T. Octupolar merocyanine dyes: a new class of nonlinear optical chromophores. *Chem. Eur. J.* **2012**, *18*, 9258–9266; d) Achelle, S.; Malval, J.-P.; Aloïse, S.; Barsella, A.; Spangenberg, A.; Mager, L.; Akdas-Kilig, H.; Fillaut, J.-L.; Caro, B.; Robin-Le Guen, F. Synthesis, photophysics and nonlinear optical properties of stilbenoid pyrimidine-based dyes bearing methylenepyran donor groups. *ChemPhysChem* **2013**, *14*, 2725–2736; e) Moreno-Yruela, C.; Garín, J.; Orduna, J.; Franco, S.; Quintero, E.; López Navarrete, J. T.; Diosdado, B. E.; Villacampa, B.; Casado, J.; Andreu, R. D- π -A compounds with tunable intramolecular charge transfer achieved by incorporation of butenolide nitriles as acceptor moieties. *J. Org. Chem.* **2015**, *80*, 12115–12128; f) Durand, R. J.; Gauthier, S.; Achelle, S.; Groizard, T.; Kahlal, S.; Saillard, J.-Y.; Barsella, A.; Le Poul, N.; Robin-Le Guen, F. Push–pull D- π -Ru- π -A chromophores: synthesis and electrochemical, photophysical and second order nonlinear optical properties. *Dalton Trans* **2018**, *47*, 3965–3975.

[11] Selected examples: a) Bolag, A.; Nishida, J.-i.; Hara, K.; Yamashita, Y. Dye-sensitized solar cells based on novel diphenylpyran derivatives. *Chem. Lett.* **2011**, *40*, 510–511; b) Pérez-Tejada, R.; Martínez de Baroja, N.; Franco, S.; Pellejà, L.; Orduna, J.; Andreu, R.;

Garín, J. Organic sensitizers bearing a trialkylsilyl ether group for liquid dye sensitized solar cells. *Dyes Pigm.* **2015**, *123*, 293–303; c) Gauthier, S.; Robin-Le Guen, F.; Wojcik, L.; Le Poul, N.; Planchat, A.; Pellegrin, Y.; Guevara Level, P.; Szuwarski, N.; Boujtita, M.; Jacquemin, D.; Odobel, F. Synthesis and properties of novel pyranilidene-based organic sensitizers for dye-sensitized solar cells. *Dyes Pigm.* **2019**, *171*, 107747; d) Andrés-Castán, J.-M.; Andreu, R.; Villacampa, B.; Orduna, J.; Franco, S. 4*H*-pyranilidene organic dyes for dye-sensitized solar cells: twisted structures towards enhanced power conversion efficiencies. *Sol. Energy* **2019**, *193*, 74–84; e) Gauthier, S.; Robin-Le Guen, F.; Wojcik, L.; Le Poul, N.; Planchat, A.; Pellegrin, Y.; Guevara Level, P.; Szuwarski, N.; Boujtita, M.; Jacquemin, D.; Odobel, F. Comparative studies of new pyranilidene-based sensitizers bearing single or double anchoring groups for dye-sensitized solar cells. *Sol. Energy* **2020**, *205*, 310–319.

[12] Guo, Z.; Zhu, W.; Tian, H. Dicyanomethylene-4*H*-pyran chromophores for OLED emitters, logic gates and optical chemosensors. *Chem. Commun.* **2012**, *48*, 6073–6084.

[13] a) Gräßler, N.; Wolf, S.; Holzmüller, F.; Zeika, O.; Vandewal, K.; Leo K. Heteroquinoid Merocyanine Dyes with High Thermal Stability as Absorber Materials in Vacuum-Processed Organic Solar Cells. *Eur. J. Org. Chem.* **2019**, 845–851; b) Tejeda-Orusco, V.; Blais, M.; Cabanetos, C.; Blanchard, P.; Andreu, R.; Franco, S.; Orduna, J.; Diosdado, B. E. 4*H*-pyranilidene-based small push-pull chromophores: Synthesis, structure, electronic properties and photovoltaic evaluation. *Dyes Pigm.* **2020**, *178*, 108357.

[14] Shen, C.; Courté, M.; Krishna, A.; Tang, S.; Fichou D. Quinoidal 2,2',6,6'-Tetraphenyl-Dipyranilidene as a Dopant-Free Hole-Transport Material for Stable and Cost-Effective Perovskite Solar Cells. *Energy Technol.* **2017**, *5*, 1852–1858.

[15] Marco, A. B.; Andreu, R.; Franco, S.; Garín, J.; Orduna, J.; Villacampa, B.; Alicante, R. Efficient second-order nonlinear optical chromophores based on dithienothiophene and thienothiophene bridges. *Tetrahedron* **2013**, *69*, 3919–3926.

- [16] a) Mandal, K.; Kar, T.; Nandi, P. K.; Bhattacharyya, S. P. Theoretical study of the nonlinear polarizabilities in H₂N and NO₂ substituted chromophores containing two hetero aromatic rings. *Chem. Phys. Lett.* **2003**, *376*, 116–124; b) Ma, X.; Ma, F.; Zhao, Z.; Song, N.; Zhang, J. Synthesis and properties of NLO chromophores with fine-tuned gradient electronic structures. *J. Mater. Chem.* **2009**, *19*, 2975–2985; c) Piao, X.; Zhang, X.; Inoue, S.; Yokoyama, S.; Aoki, I.; Miki, H.; Otomo, A.; Tazawa, H. Enhancement of electro-optic activity by introduction of a benzyloxy group to conventional donor- π -acceptor molecules. *Org. Electron.* **2011**, *12*, 1093–1097.
- [17] Liu, F.; Chen, S.; Mo, S.; Qin, G.; Yu, C.; Zhang, W.; Shi, W.-J.; Chen, P.; Xu, H.; Fuc, M. Synthesis of novel nonlinear optical chromophores with enhanced electro-optic activity by introducing suitable isolation groups into the donor and bridge. *J. Mater. Chem. C* **2019**, *7*, 8019–8028.
- [18] Ford, J. A., Jr.; Wilson, C. V.; Young, W. R. The Preparation of 2(5*H*)-Furanones and Dyes Derived from Them. *J. Org. Chem.* **1967**, *32*, 173–177.
- [19] Melikian, G.; Rouessac, F. P.; Alexandre, C. Synthesis of Substituted Dicyanomethylenedihydrofurans. *Synth. Commun.* **1995**, *25*, 3045–3051.
- [20] a) Conditions for acceptors **3** y **5**: Marco, A. B.; Martínez de Baroja, N.; Franco, S.; Garín, J.; Orduna, J.; Villacampa, B.; Revuelto, A.; Andreu, R. Dithienopyrrole as a Rigid Alternative to the Bithiophene π -Relay in Chromophores with Second-Order Nonlinear Optical Properties. *Chem. Asian J.* **2015**, *10*, 188–197; b) conditions for acceptor **4**: Reference 10e.
- [21] a) Gauthier, S.; Caro, B.; Robin-Le Guen, F.; Bhuvanesh, N.; Gladysz, J. A.; Wojcik, L.; Le Poul, N.; Planchat, A.; Pellegrin, Y.; Blart, E.; Jacquemin, D.; Odobel, F. Synthesis, photovoltaic performances and TD-DFT modeling of push–pull diacetylide platinum complexes in TiO₂ based dye-sensitized solar cells. *Dalton Trans* **2014**, *43*, 11233–11242; b)

Durand, R. J.; Gauthier, S.; Achelle, S.; Kahlal, S.; Saillard, J.-Y.; Barsella, A.; Wojcik, L.; Le Poul, N.; Robin-Le Guen, F. Incorporation of a platinum center in the pi-conjugated core of push–pull chromophores for nonlinear optics (NLO). *Dalton Trans* **2017**, *46*, 3059–3069;

c) Gauthier, S.; Porter, A.; Achelle, S.; Roisnel, T.; Dorcet, V.; Barsella, A.; Le Poul, N.; Guevara Level, P.; Jacquemin, D.; Robin-Le Guen, F. Mono- and Diplatinum Polyynediyl Complexes as Potential Push–Pull Chromophores: Synthesis, Characterization, TD-DFT Modeling, and Photophysical and NLO Properties. *Organometallics* **2018**, *37*, 2232–2244.

[22] a) Koeckelberghs, G.; De Groof, L.; Pérez-Moreno, J.; Asselberghs, I.; Clays, K.; Verbiest, T.; Samyn, C. Synthesis and nonlinear optical properties of linear and Λ -shaped pyranone-based chromophores. *Tetrahedron* **2008**, *64*, 3772–3781; b) Achelle, S.; Kahlal, S.; Saillard, J.-Y.; Cabon, N.; Caro, B.; Robin-Le Guen, F. Dipolar and V-shaped structures incorporating methylenepyran and diazine fragments. *Tetrahedron* **2014**, *70*, 2804–2815.

[23] a) Kim, O.-K.; Fort, A.; Barzoukas, M.; Blanchard-Desce, M.; Lehn, J.-M. Nonlinear optical chromophores containing dithienothiophene as a new type of electron relay. *J. Mater. Chem.* **1999**, *9*, 2227–2232; b) Ma, X.; Ma, F.; Zhao, Z.; Song N.; Zhang, J. Toward highly efficient NLO chromophores: Synthesis and properties of heterocycle-based electronically gradient dipolar NLO chromophores. *J. Mater. Chem.* **2010**, *20*, 2369–2380; c) Kalinin, A. A.; Sharipova, S. M.; Burganov, T. I.; Dudkina, Y. B.; Khamatgalimov, A. R.; Katsyuba, S. A.; Budnikova, Y. H.; Balakina, M. Y. Push-pull isomeric chromophores with vinyl- and divinylquinoxaline-2-one units as π -electron bridge: Synthesis, photophysical, thermal and electro-chemical properties. *Dyes Pigm.* **2017**, *146*, 82–91.

[24] Jacquemin, D.; Wathélet, V.; Perpète, E. A.; Adamo, C. Extensive TD-DFT Benchmark: Singlet-Excited States of Organic Molecules. *J. Chem. Theory Comput.* **2009**, *5*, 2420–2435.

[25] a) Oudar, J. L.; Chemla, D. S. Hyperpolarizabilities of nitroanilines and their relations to excited-state dipole moment. *J. Chem. Phys.* **1977**, *66*, 2664–2668; b) Kanis, D. R.; Ratner M.

A.; Marks, T. J. Design and construction of molecular assemblies with large 2nd order optical nonlinearities- Quantum chemical aspects. *Chem. Rev.* **1994**, *94*, 195–242.

[26] Champagne, B.; Perpète, E. A.; Jacquemin, D.; van Gisbergen, S. J. A.; Baerends, E.-J.; Soubra-Ghaoui, C.; Robins, K. A.; Kirtman, B. Assessment of Conventional Density Functional Schemes for Computing the Dipole Moment and (Hyper)polarizabilities of Push-Pull π -Conjugated Systems. *J. Phys. Chem. A* **2000**, *104*, 4755–4763.

[27] In this model, the first hyperpolarizability β value of the chromophores is proportional to the parameters showed in the formula. $\Delta\mu_{01}$ is the difference between the dipole moment of the ground state (0) and the excited state (1) of the molecule, μ_{01} is the dipole moment of the transition, and E_{01} is the energy gap between the ground (0) and excited states (1) of the molecules.

$$\beta \propto \frac{\mu_{01}^2 \Delta\mu_{01}}{E_{01}^2} \propto \frac{f \Delta\mu_{01}}{E_{01}^3}$$

[28] Moylan, C. R.; Ermer, S.; Lovejoy, S. M.; McComb, I.-H.; Leung, D. S.; Wortmann, R.; Krdmer, P.; Twieg, R. J. (Dicyanomethylene)pyran Derivatives with C_{2v} Symmetry: An Unusual Class of Nonlinear Optical Chromophores. *J. Am. Chem. Soc.* **1996**, *118*, 12950–12955.

[29] Franco, S.; Garín, J.; Martínez de Baroja, N.; Pérez-Tejada, R.; Orduna, J.; Yu, Y.; Lira-Cantú, M. New D- π -A-conjugated organic sensitizers based on 4*H*-pyran-4-ylidene donors for highly efficient dye-sensitized solar cells. *Org. Lett.* **2012**, *14*, 752–755.

[30] a) Ba, F.; Cabon, N.; Le Poul, P.; Kahlal, S.; Saillard, J.-Y.; Le Poul, N.; Golhen, S.; Caro, B.; Robin-Le Guen, F. Diferrocenylpyrylium salts and electron rich bispyran from oxidative coupling of ferrocenylpyran. Example of redox systems switched by proton transfer. *New J. Chem.* **2013**, *37*, 2066–81; b) Gauthier, S.; Vologdin, N.; Achelle, S., Barsella, A.; Caro, B.; Robin-Le Guen F. Methylene-pyran based dipolar and quadrupolar dyes: synthesis,

electrochemical and photochemical properties. *Tetrahedron* **2013**, *69*, 8392–8399; c) Novoa, N.; Roisnel, T.; Dorcet, V.; Hamond, J.-R.; Carrillo, D.; Manzur, C.; Robin-Le Guen, F.; Cabon, N. Anisyl and ferrocenyl adducts of methylenepyran-containing β -diketone: Synthesis, spectral, structural, and redox properties. *J. Organomet. Chem.* **2014**, *762*, 19–28; d) Le Poul, P.; Le Poul, N.; Golhen, S.; Robin-Le Guen, F.; Caro B. The synthesis of flexible tetrapyridylethanes from pyridylpyrylium dications. *New J. Chem.* **2016**, *40*, 5666–5669; e) Wojcik, L.; Michaud, F.; Gauthier, S.; Cabon, N.; Le Poul, P.; Gloaguen, F.; Le Poul, N. Reversible Redox Switching of Chromophoric Phenylmethylenepyranes by Carbon–Carbon Bond Making/Breaking. *J. Org. Chem.* **2017**, *82*, 12395–12405.

[31] Bourhill, G.; Brédas, J.-L.; Cheng, L.-T.; Marder, S. R.; Meyers, F.; Perry, J. W.; Tiemann, B. G. Experimental Demonstration of the Dependence of the First Hyperpolarizability of Donor-Acceptor-Substituted Polyenes on the Ground-State Polarization and Bond Length Alternation. *J. Am. Chem. Soc.* **1994**, *116*, 2619–2620.

[32] Dirk, C. W.; Katz, H. E.; Schilling, M. L.; King, L. A. Use of Thiazole Rings To Enhance Molecular Second-Order Nonlinear Optical Susceptibilities. *Chem. Mater.* **1990**, *2*, 700–705.

[33] Gaussian 16, Revision A.03, Frisch, M. J.; Trucks, G. W.; Schlegel, H. B.; Scuseria, G. E.; Robb, M. A.; Cheeseman, J. R.; Scalmani, G.; Barone, V.; Petersson, G. A.; Nakatsuji, H.; Li, X.; Caricato, M.; Marenich, A. V.; Bloino, J.; Janesko, B. G.; Gomperts, R.; Mennucci, B.; Hratchian, H. P.; Ortiz, J. V.; Izmaylov, A. F.; Sonnenberg, J. L.; Williams-Young, D.; Ding, F.; Lipparini, F.; Egidi, F.; Goings, J.; Peng, B.; Petrone, A.; Henderson, T.; Ranasinghe, D.; Zakrzewski, V. G.; Gao, J.; Rega, N.; Zheng, G.; Liang, W.; Hada, M.; Ehara, M.; Toyota, K.; Fukuda, R.; Hasegawa, J.; Ishida, M.; Nakajima, T.; Honda, Y.; Kitao, O.; Nakai, H.; Vreven, T.; Throssell, K.; Montgomery, J. A., Jr.; Peralta, J. E.; Ogliaro, F.; Bearpark, M. J.; Heyd, J. J.; Brothers, E. N.; Kudin, K. N.; Staroverov, V. N.; Keith, T. A.;

Kobayashi, R.; Normand, J.; Raghavachari, K.; Rendell, A. P.; Burant, J. C.; Iyengar, S. S.; Tomasi, J.; Cossi, M.; Millam, J. M.; Klene, M.; Adamo, C.; Cammi, R.; Ochterski, J. W.; Martin, R. L.; Morokuma, K.; Farkas, O.; Foresman, J. B.; Fox, D. J. Gaussian, Inc., Wallingford CT, 2016.

[34] Barone, V.; Cossi, M. Quantum calculation of molecular energies and energy gradients in solution by a conductor solvent model. *J. Phys. Chem. A* **1998**, *102*, 1995–2001.

[35] Cossi, M.; Rega, N.; Scalmani, G.; Barone, V. Energies, structures, and electronic properties of molecules in solution with the C-PCM solvation model. *J. Comput. Chem.* **2003**, *24*, 669–681.

[36] Zhao, Y.; Truhlar, D. G. The M06 suite of density functionals for main group thermochemistry, thermochemical kinetics, noncovalent interactions, excited states, and transition elements: two new functionals and systematic testing of four M06-class functionals and 12 other functionals. *Theor. Chem. Acc.* **2008**, *120*, 215–241.

[37] Hariharan, P. C.; Pople, J. A. Influence of polarization functions on MO hydrogenation energies. *Theor. Chim. Acta* **1973**, *28*, 213–222.

[38] Hanwell, M. D.; Curtis, D. E.; Lonie, D. C.; Vandermeersch, T.; Zurek, E.; Hutchison, G. R. Avogadro: an advanced semantic chemical editor, visualization, and analysis platform. *J. Cheminf.* **2012**, *4*, 17.

For Table of Contents Only

